Warming winters in lakes: Later ice onset promotes consumer overwintering and shapes springtime planktonic food webs

Marie-Pier Hébert[a,b,c,1], Beatrix E. Beisner[b,c], Milla Rautio[c,d], and Gregor F. Fussmann[a,c]

[a]Department of Biology, McGill University, Montréal, QC H3A 1B1, Canada; [b]Département des Sciences Biologiques, Université du Québec à Montréal, Montréal, QC H3C 3P8, Canada; [c]Groupe de Recherche Interuniversitaire en Limnologie, QC, Canada; and [d]Département des Sciences Fondamentales, Université du Québec à Chicoutimi, Chicoutimi, QC G7H 2B1, Canada

Edited by Nils Chr. Stenseth, Universitetet i Oslo, Oslo, Norway, and approved October 21, 2021 (received for review August 12, 2021)

Global climate warming is causing the loss of freshwater ice around the Northern Hemisphere. Although the timing and duration of ice covers are known to regulate ecological processes in seasonally ice-covered ecosystems, the consequences of shortening winters for freshwater biota are poorly understood owing to the scarcity of under-ice research. Here, we present one of the first in-lake experiments to postpone ice-cover onset (by ≤21 d), thereby extending light availability (by ≤40 d) in early winter, and explicitly demonstrate cascading effects on pelagic food web processes and phenologies. Delaying ice-on elicited a sequence of events from winter to spring: 1) relatively greater densities of algal resources and primary consumers in early winter; 2) an enhanced prevalence of winter-active (overwintering) consumers throughout the ice-covered period, associated with augmented storage of high-quality fats likely due to a longer access to algal resources in early winter; and 3) an altered trophic structure after ice-off, with greater initial springtime densities of overwintering consumers driving stronger, earlier top-down regulation, effectively reducing the spring algal bloom. Increasingly later ice onset may thus promote consumer overwintering, which can confer a competitive advantage on taxa capable of surviving winters upon ice-off; a process that may diminish spring food availability for other consumers, potentially disrupting trophic linkages and energy flow pathways over the subsequent open-water season. In considering a future with warmer winters, these results provide empirical evidence that may help anticipate phenological responses to freshwater ice loss and, more broadly, constitute a case of climate-induced cross-seasonal cascade on realized food web processes.

global climate warming | freshwater ice loss | phenology | trophic interactions | winter limnology

Global climate warming increases surface water temperature (1, 2), causing widespread loss of freshwater ice cover across the Northern Hemisphere (3, 4). Long-term records indicate that freshwater ecosystems at higher latitudes experience accelerating rates of warming, with strong trends of increasingly later ice-on, earlier ice-off, and shorter duration of seasonal ice covers (5–8). Pronounced changes in the timing and duration of ice-covered seasons are bound to have far-reaching ecological consequences (9). Yet, freshwater ecology remains relatively understudied in winter, especially when compared with marine research (10–13). Although ice phenology and some remotely sensed abiotic measures have been well-documented in lakes and rivers (3, 8, 10), under-ice assessments of biota are considerably limited. As a result, the effects of rapidly changing winters on freshwater food webs and biological processes remain largely unknown, impeding our ability to anticipate the implications of ice loss.

The ice-covered period has long been perceived as a dormant season for freshwater organisms, especially in lakes (12). Recent studies challenged this prevailing view, suggesting that critical processes can occur under ice (14, 15), with the timing and physical features of ice covers driving dynamics in winter, spring, and possibly over the summer (12, 16, 17). Indeed, while several freshwater taxa may favor dormancy in winter, certain environmental conditions (e.g., light, food availability) and organismal traits (e.g., thermal tolerance) may allow communities to remain active under ice. For example, motile phytoplankton with flexible forms of nourishment—such as mixotrophic phytoflagellates—may prevail in winter (18, 19), remaining in suspension despite the absence of water mixing under ice and shifting their nutritional mode from photosynthesis to partially or fully utilizing organic sources of carbon when light availability is reduced. Pelagic primary consumers may also benefit from relaxed predation in winter, with reports of active, abundant, and, even, reproducing zooplankton populations (20–22). Active overwintering, however, may impose a long period of limited resources on consumers. For instance, energetically rewarding, photosynthetic prey can become rare in winter, compelling zooplankton to rely on other survival strategies to overcome nutritional shortage, such as using previously accumulated high-quality fat reserves (20, 23, 24) or shifting their diet to incorporate alternative, lower-quality resources of bacterial or terrestrial origin (19, 25).

Significance

Freshwater ice is being lost at an accelerating rate with global warming. Yet the ecological implications of shortening ice-covered seasons remain largely unexplored due to a historical lack of freshwater research in winter. We provide an innovative experimental study that realistically reproduces warming effects on the timing of ice onset to address the consequences for lake food webs. We find that later ice-on sustains photosynthesis longer, permitting greater accumulation of high-quality fat reserves in primary consumers, and likely facilitating winter survival. Further, we show that a greater prevalence of overwintering consumers shapes springtime food webs via an increased top-down control of the spring algal bloom. Broadly, this study demonstrates that warmer winters can have cross-seasonal cascading effects on ecological processes.

Author contributions: M.-P.H. performed the research, analyzed data, and wrote and revised the paper; and M.-P.H., B.E.B., M.R., and G.F.F. discussed the study, contributed materials or analytic tools, and approved the manuscript.

The authors declare no competing interest.

This article is a PNAS Direct Submission.

[1]To whom correspondence may be addressed. Email: mphebert4@gmail.com.

This article contains supporting information online at http://www.pnas.org/lookup/suppl/doi:10.1073/pnas.2114840118/-/DCSupplemental.

Published November 22, 2021.

As ice-on dates trend later with climate warming, prolonged light exposure in early winter may sustain photosynthesis and energy-rich resource availability longer, permitting greater accumulation of algal-derived fat reserves in primary consumers. Extending the time period during which zooplankton can store high-quality fats may in turn enhance active overwintering. Shorter seasonal duration of ice cover could also facilitate winter survival, reducing the period during which consumers may rely on previously accumulated fat storage. A greater prevalence of winter-active consumers could, however, trigger strong cascading effects on trophic interactions upon ice breakup, including reduced spring algal blooms or greater mismatches in the timing of resource and consumer growth [phenological decoupling (26–30)]. Enhanced winter survival in consumers could also promote the co-occurrence of competing taxa in spring, resulting in earlier and possibly greater competition for limited resources (31). Thus, the timing of ice-cover onset may represent a key determinant of consumer winter strategies and food web interactions at the beginning of the open-water season, a question that remains hitherto unanswered owing to the paucity of empirical data on under-ice freshwater food webs.

To explicitly test how later ice-on may affect winter survival in pelagic primary consumers and springtime planktonic food webs, we performed an in situ experimental study to manipulate the timing of ice-cover onset using in-lake enclosures. Exploiting a floating facility deployed on a temperate lake in eastern Canada (45°32′N, 73°08′W), we filled 16 pelagic enclosures with *ca*. 3,400 L of lake water and planktonic organisms at the beginning of the ice-covered period (Fig. 1 *A*–*C*) and postponed the onset of naturally forming ice cover by 0, 7, 14, and 21 d (Fig. 1*D*),

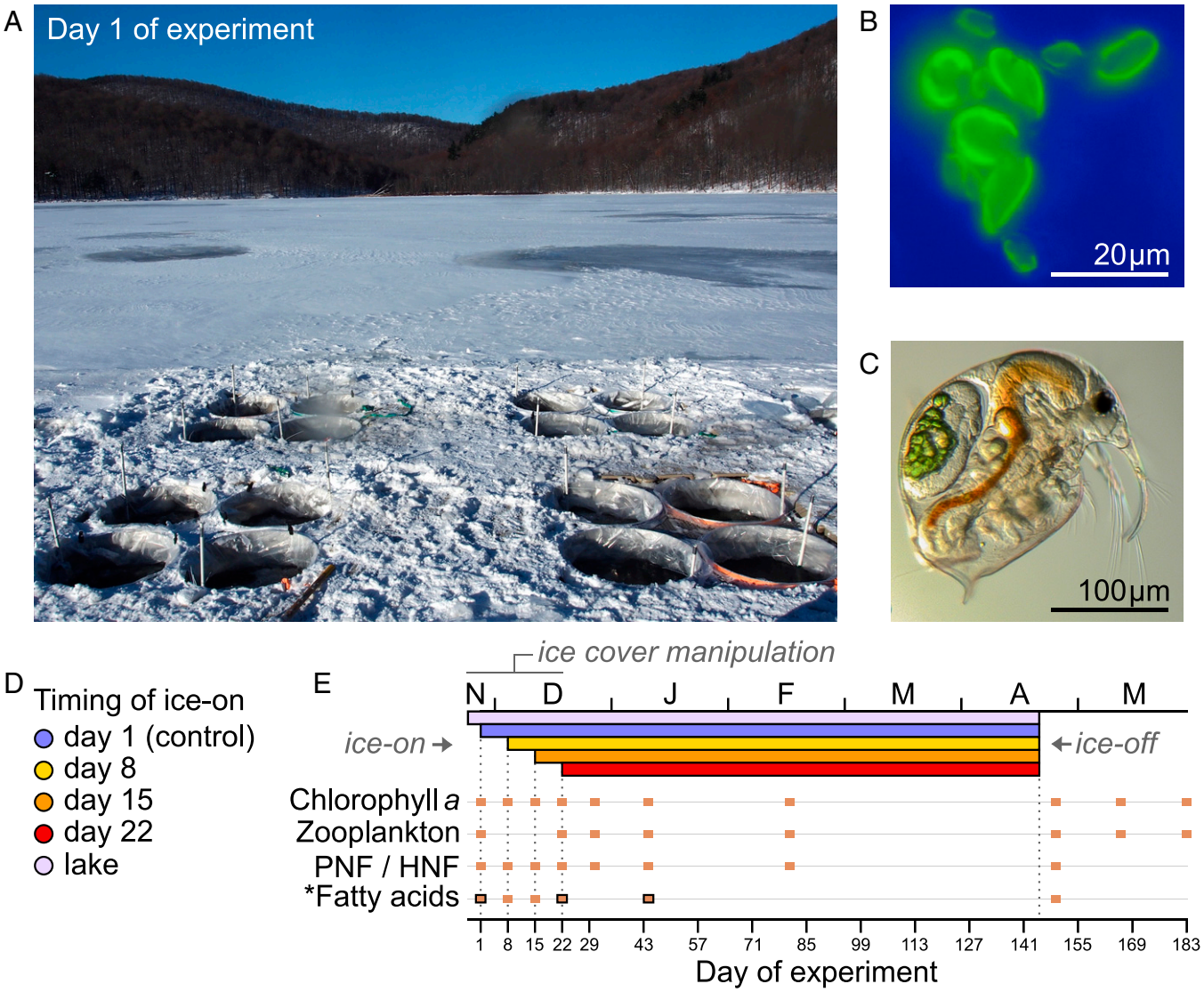

Fig. 1. In-lake experimental setup, under-ice organisms, design, and timeline. (*A*) The floating platform deployed on Lac Hertel (Mont Saint-Hilaire, Québec), accommodating 16 enclosures (depth *ca*. 4.2 m), each containing *ca*. 3,400 L of lake water and planktonic organisms. (*B* and *C*) Microscope photographs of under-ice plankton in early winter: (*B*) phototrophic nanophytoflagellates (*Cryptophyceae*; epifluorescence microscopy) and (*C*) crustacean zooplankton (*Bosmina*). (*D* and *E*) Schematic representation of ice-cover treatments and timeline. Colors refer to treatment levels of ice-cover manipulation, indicating the (*D*) timing of ice-cover formation onset across enclosures and (*E*) resulting ice-covered periods. Lac Hertel's ice-covered period is illustrated as a frame of reference. (*E*) Symbols indicate sampling days over the course of the 183-d experiment. Biotic response variables include total and group-specific chl-*a* concentrations, crustacean and rotifer zooplankton densities, fully or partially phototrophic (PNF) and heterotrophic/phagotrophic (HNF) nanoflagellates, and characterization of FAs in zooplankton and seston. Upper and lower horizontal axes indicate time of the year and day of experiment, respectively. Temporal dynamics of light incidence and other baseline measurements are provided in *SI Appendix*, with additional details in *Materials and Methods*. *FAs were characterized on six occasions for seston (filled symbols) and on three occasions for zooplankton (framed symbols) (see details in *Materials and Methods*).

resulting in contrasting light-incidence patterns over a period up to 40 d (*SI Appendix*, Fig. S1). We recorded a variety of biotic responses over 183 d through winter and spring (Fig. 1*E*) to address whether delayed ice-on dates and prolonged light exposure can: 1) sustain photosynthesis longer and allow pelagic multitrophic communities (algal resources and zooplankton consumers) to maintain high densities in early winter; 2) enhance the prevalence of overwintering consumers over the winter months, and whether winter survival is linked to early-winter fat accumulation and/or shifts in dietary supply sources; and 3) elicit cascading effects on the structure of springtime planktonic food webs, both across and within trophic levels (i.e., consumer–resource and consumer–consumer relationships).

Results and Discussion

Systematically removing freshly formed ice in enclosures twice per day over up to 21 d, our approach effectively postponed the establishment of ice cover, resulting in four evenly spaced ice-on dates: days 1 (control), 8, 15, and 22 of the experiment. Following ice-cover onset, rates of under-ice light attenuation varied among enclosures with different ice-on dates owing to fluctuations in local weather conditions (*Materials and Methods* and *SI Appendix*, Fig. S1). Specifically, light availability declined relatively rapidly after ice-cover formation on days 1 and 8 due to subsequent snowfall. In contrast, under-ice light attenuation occurred more slowly where ice was allowed to form on day 15, in part owing to mild weather and lack of snow cover (until day 21). As a result, light-incidence patterns were similar across enclosures with ice-cover onset on days 15 and 22, receiving on average >200% more light than controls at a 1-m depth during the treatment period (days 1 to 22). Upon completion of ice manipulations (day >22), carry-over effects were observable until day 40, with sustained greater under-ice light availability mainly detected in enclosures with day 22 ice-on dates (*SI Appendix*, Fig. S1 and Table S1). Experimentally delaying ice-cover onset did not affect water temperature, indicating that biotic responses to our manipulations were likely caused by light-regime differences (*SI Appendix*, Table S2).

A linear mixed-effects model (LMM) revealed that later ice-on dates positively affected chlorophyll *a* (chl-*a*) concentrations in early winter, with chl-*a* declining more slowly where ice-on was delayed (Fig. 2 *A* and *E*). These trends were primarily driven by cryptophytes (Fig. 1*B* and *SI Appendix*, Fig. S3*A*), a group of mixotrophic nanophytoflagellates capable of both phototrophy (autotrophy) and phagotrophy (heterotrophy) (32). A finer examination by epifluorescence microscopy of the relative proportions of phototrophic nanoflagellates (pigmented cells; PNFs) versus heterotrophic/phagotrophic nanoflagellates (nonpigmented cells; HNFs) indicated that PNF:HNF mass ratios remained higher with later ice-on (Fig. 2 *B* and *E*). This result suggests a postponed metabolic shift from autotrophy/mixotrophy to full heterotrophy for nanoflagellates and, thus, longer access to photosynthetic (energetically rewarding) prey for consumers. After ice-cover formation, both chl-*a* concentrations and PNF:HNF ratios decreased similarly across enclosures. Overall, our ice-cover manipulation strongly influenced algal availability for a nonnegligible period of ≤45 d (Fig. 2 *A*, *B*, and *E*), coinciding with the extended light availability period where ice-on was most delayed (*SI Appendix*, Fig. S1). Thus, changes in light incidence in early winter, before and after ice-cover onset, can drive chl-*a* levels and metabolic (nutritional) shifts at the base of the food chain and, by extension, the quantity and quality of algal resources available during a critical seasonal transition.

The primary consumers in our enclosures, rotifer and crustacean zooplankton, showed contrasting temporal trends in early winter: rotifers visibly proliferated until day 45, while crustaceans progressively declined over time (Fig. 2 *C* and *D*). Rotifers appeared to be naturally active under ice, reaching impressively high densities. Postponing ice-cover onset strengthened their biomass increases on day 45, likely due to greater food availability (with corresponding declines in chl-*a* thereafter; Fig. 2*A*), but did not affect their survivorship later in winter (Fig. 2*E*). Although often neglected in freshwater biotic assessments, abundant rotifer communities have been previously reported during winter, when they are thought to benefit from reduced competition and predation (33–35). For crustaceans, biomass levels remained generally higher in enclosures with later ice-on, with lagged positive responses to treatment detected on days 45 and 81 (Fig. 2 *D* and *E*). Crucially, the presence of greater crustacean densities on day 81 where ice covers formed on days 15 and 22 constitutes evidence of long-lasting effects of later lake ice onset on consumer winter survival. Although crustaceans of the genus *Bosmina* maintained high densities in early winter (Fig. 1*C* and *SI Appendix*, Fig. S4*C*), with positive effects of delayed ice-on captured on day 45, long-term winter survival was only observed in cyclopoid copepods, mainly *Cyclops*, a taxon known to overwinter [*SI Appendix*, Fig. S4*A* (19, 20, 23)].

To evaluate whether the timing of ice-cover onset influenced consumer winter survival strategies, we examined the signatures of fatty acids (FAs) accumulated in zooplankton and seston across enclosures. Seston refers to suspended organisms and materials between 0.7 and 53 μm (i.e., algae, microzooplankton, larger bacteria, particulate debris), and hence representative of zooplankton food sources. In addition to being essential for consumer dietary requirements, FAs are important for energy storage (36, 37). As such, we quantified the levels of 40 individual FAs and used FA signatures as a proxy to address whether ice-on dates influenced 1) the composition of zooplankton fats and 2) their dietary (energy) supply source in early winter, focusing on days 22 and 45. A nonmetric multidimensional scaling (NMDS) revealed that zooplankton communities from treated enclosures exhibited distinct FA composition as early as day 22 (Fig. 3*A*). A permutational multivariate analysis of variance (PERMANOVA) confirmed that the timing of ice-on explained differences in zooplankton FA composition [$P = 0.013$, $F_{(1,15)} = 3.149$]. However, this effect was not captured on day 45 (*SI Appendix*, Fig. S5*A*), possibly as a result of missing values from enclosures with later ice-on (*Materials and Methods*). In contrast, our ice-cover manipulation had no discernable effects on seston FA composition on day 22, nor on day 45 (*SI Appendix*, Fig. S5 *C* and *E*), suggesting that zooplankton FA composition did not reflect that of seston.

Building on previous studies exploiting the use of FAs as biomarkers to trace energy sources, we identified the origin of FAs for which this was possible (23 out of the 40 FAs quantified) and estimated FA proportions derived from algal, terrestrial, and bacterial biosynthesis in zooplankton and seston (see *Materials and Methods* and references therein). By the end of the treatment period, both absolute amounts and proportions (% relative to total FAs) of algal-derived FAs had largely increased in zooplankton where ice-on was delayed (Fig. 3*B* and *SI Appendix*, Table S3), constituting up to 12.4% (±1.98) of zooplankton FAs, in contrast to 5.6% (±1.76) in controls. With later ice-on, terrestrially derived FAs also increased in zooplankton but their low relative importance (<1%) suggests that zooplankton primarily accumulated algal FAs in early winter. On day 45, up to 23.1% (±5.52) of zooplankton FAs were algal-derived (*SI Appendix*, Fig. S5*B*); however, effects of ice-on dates were statistically undetectable, again possibly owing to missing FA values (*Materials and Methods*). Further refining our examination, we targeted specific essential, algal-derived FAs known to be associated with seasonal physiological regulation in zooplankton [i.e., docosahexaenoic acid (DHA), arachidonic acid (ARA), eicosapentaenoic acid (EPA) (36, 38)], and found that zooplankton DHA and ARA levels increased with

ECOLOGY

later ice-on (*SI Appendix*, Table S3). Notably, on day 45, we measured markedly greater proportions of DHA in zooplankton where ice formed on day 22, constituting alone 7.91% (±0.51) of total FAs and representing a 2.8× increase relative to control communities (*SI Appendix*, Fig. S5*B*). Thus, accumulating algal-derived FAs (such as DHA) in early winter appears to be a key complementary strategy employed by overwintering zooplankton, predominantly cyclopoid copepods in our enclosures (*SI Appendix*, Fig. S4*A*).

For seston, delayed ice-cover onset increased ARA levels on day 22 and total algal-derived FAs, especially DHA, on day 45 (*SI Appendix*, Table S4). Despite these trends, seston FAs failed to predict FA accumulation in zooplankton; only % ARA similarly increased in both seston and zooplankton on day 22 (P = 0.039), although levels remained <1% (*SI Appendix*, Table S5). Our inability to link zooplankton and seston FA composition suggests that overwintering consumers may have preferentially retained specific FAs in early winter, a strategy previously observed in overwintering freshwater copepods [*SI Appendix*, Fig. S6 (20, 21, 23)]. That is, as zooplankton store high-quality FAs at different rates (i.e., selective accumulation of algal-derived FAs, especially DHA and, to a lesser extent, ARA, in this case), the lack of relationship between seston and zooplankton FA composition may be expected (24, 38), especially if selective feeders such as copepods dominate under-ice communities.

We further quantified the effects of later ice onset on springtime planktonic food webs, tracking temporal dynamics over *ca*. 1 mo after ice-off (days 150 to 183). On days 150 (a few days after ice melt) and 166, we found greater crustacean densities where ice-on was delayed and enhanced overwintering occurred (Fig. 2 *D* and *E*). Crustacean communities in early spring were primarily composed of cyclopoid copepods (*SI Appendix*, Fig. S4*A*), confirming their survival through winter. Cladoceran densities were low, slowly increasing as photoperiods became longer. While rotifers could survive the winter under ice, their spring biomass was generally low, showing no clear differences among enclosures. In stark contrast, chl-*a* concentrations were distinctly lower where ice-on was delayed (Fig. 2*A*). A LMM validated that our ice-cover manipulation had a time-dependent effect on chl-*a*, shifting from positive in early winter to negative after ice-off (likely mediated by trophic interactions; Fig. 2*E*). Spring trends in chl-*a* were mainly driven by green algae (*SI Appendix*, Fig. S3). While differences were still observable at fine taxonomic scales on day 183, effects on both total crustaceans and chl-*a* became undetectable, coinciding with the emergence and population growth of other crustacean taxa that likely resulted in more complex species interactions (*SI Appendix*, Fig. S4).

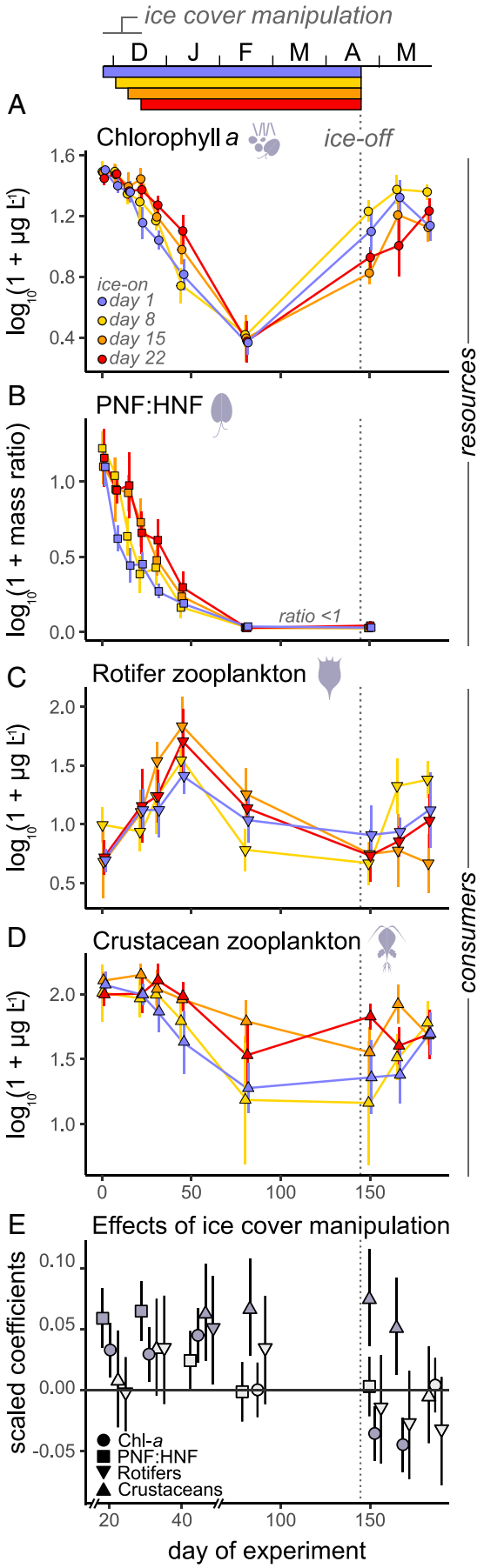

Fig. 2. Temporal effects of ice-cover manipulation on planktonic food webs. (*A*–*D*) Time series of (*A*) total chl-*a* concentrations (circle), (*B*) carbon mass ratios between photosynthetic and heterotrophic nanoflagellates (PNF:HNF; square), and (*C*) rotifer (inverted triangle) and (*D*) crustacean (triangle) zooplankton biomass over the experiment. Colors indicate ice-cover treatment levels. Error bars represent 95% CIs. Shaded gray areas illustrate the overall treatment period (i.e., days 1 to 22); note that carry-over effects on light availability were observable until ca. day 40. Dashed lines indicate the timing of ice breakup (concomitant across all enclosures). A slight offset on *x* axis values was introduced to facilitate data visualization. Temporal effects at finer taxonomic scales are provided in *SI Appendix*, Figs. S3 and S4. (*E*) Time-dependent effects of ice-cover manipulation on planktonic food webs. LMMs were performed individually for each plankton group. Effect sizes are expressed as scaled parameter estimates of LMMs, quantified as of the end of the treatment period, namely days 22, 31, 45, 81, 150, 166, and 183. Error bars represent 95% CIs. Treatment effects are significant ($P < 0.05$) when error bars do not overlap with the zero line; filled and shaded symbols represent significant and nonsignificant effects, respectively. To facilitate visualization between days 22 and 45, two breaks and a larger offset were introduced on *x* axis values.

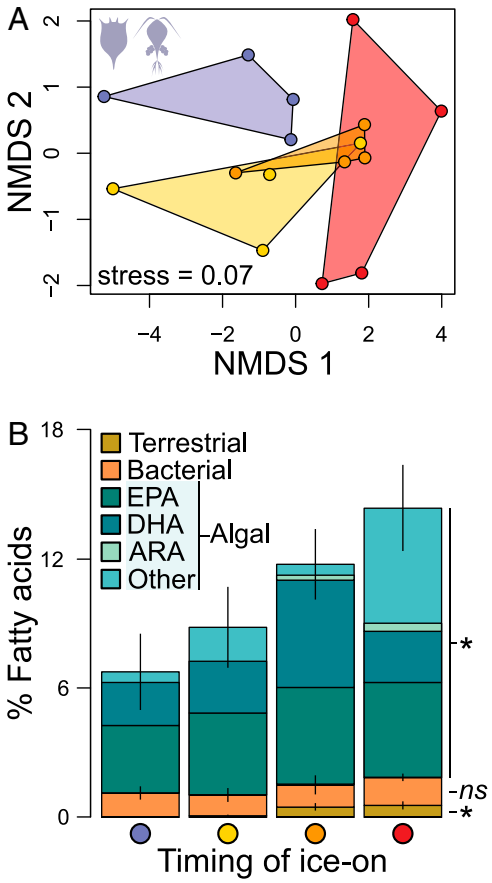

Fig. 3. Effects of ice-cover manipulation on primary consumer FA composition in early winter. (*A*) NMDS representation of zooplankton FA composition on day 22 (i.e., end of treatment period) using all quantified FAs ($\mu g \cdot mg^{-1}$ dry mass). Convex hulls illustrate differences in FA composition among ice-cover treatments and colors refer to treatment levels; the legend is as in Figs. 1 and 2. (*B*) Proportions of FA biomarkers (% relative to all FAs) derived from algal (green), bacterial (orange), and terrestrial (brown) sources accumulated in zooplankton on day 22. Asterisks denote significant effects ($P < 0.05$) of ice-cover manipulation on source-specific FA biomarkers; *ns*, not significant. Error bars indicate SEs. Proportions of EPA, DHA, and ARA are represented within algal FA biomarkers. *SI Appendix*, Table S3 includes model coefficients for all tested FA components for days 22 and 45.

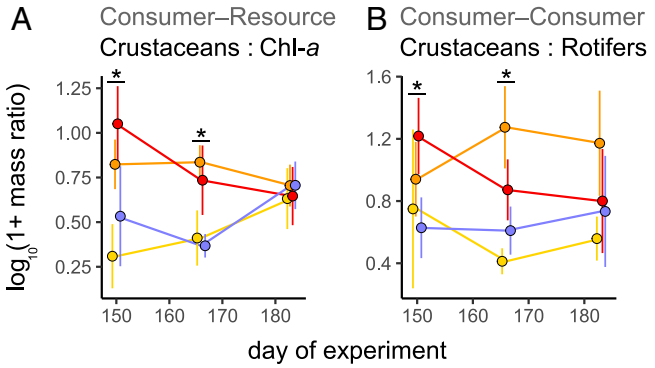

Fig. 4. Cascading effects of crustacean winter survival on springtime food web structure. Mass ratios between crustacean densities and (*A*) chl-*a* concentration and (*B*) rotifer densities over 33 d after ice breakup (days 150 to 183). Error bars represent 95% CIs. Asterisks denote significant effects ($P < 0.05$) of ice-cover manipulation on mass ratios (measured as parameter estimates of LMMs). Variations in crustacean densities are primarily driven by overwintering copepods in spring (*SI Appendix*, Fig. S7).

To more directly test whether consumer winter survival affected trophic structure after ice-off, we explored consumer–resource relationships. Where overwintering was enhanced, crustacean-to-chl-*a* mass ratios were substantially higher in spring (Fig. 4*A*). As a common indicator of resource-use efficiency in lakes (e.g., ref. 39), greater mass ratios between zooplankton and chl-*a* can indicate stronger top-down effects. Neither cladoceran-to-chl-*a* nor rotifer-to-chl-*a* ratios showed differences; only consumer–resource ratios including cyclopoid copepods increased with later ice-on (*SI Appendix*, Fig. S7), suggesting an important role of overwintering copepods in controlling the spring algal bloom.

Comparing mass ratios between springtime densities of overwintering consumer taxa as a proxy for competition, we found that crustacean biomass, mainly cyclopoid copepods, was also significantly higher than rotifer biomass in enclosures where ice-on was delayed (Fig. 4*B* and *SI Appendix*, Fig. S7). Greater consumer–consumer mass ratios in favor of overwintering copepods could indicate that they outcompeted or, even, preyed upon rotifers; however, given that spring rotifer densities were not greater in controls (where copepod densities were lower; Fig. 2 *C–E*), our data suggest that rotifer densities were unaffected by overwintering copepods. Although winter survival in both copepods and rotifers did not result in competitive exclusion at the beginning of the open-water season, the concomitance of higher crustacean-to-chl-*a* and crustacean-to-rotifer ratios suggests that springtime planktonic food webs may be relatively more top-heavy (i.e., shaped into an inverted biomass pyramid) when crustaceans such as cyclopoids overwinter.

Manipulating the timing of ice-cover onset (over ≤21 d) and prolonging light availability (by ≤40 d) under realistic environmental conditions in early winter, our experimental study provides evidence that causally links later ice-on to consumer overwintering, with cascading effects on the structure and processes of springtime food webs. Our main findings and hypothesized

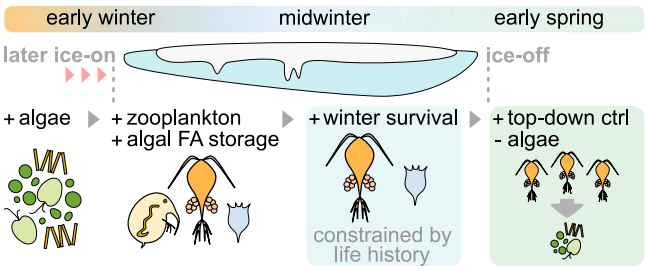

Fig. 5. Schematic summary of potential direct and indirect effects of later ice-cover onset on lake planktonic food webs, from early winter to spring. Positive and negative effects are denoted via "+" and "−" signs; the ice-covered period is illustrated by the ice cover. Short-term effects of later ice-on dates include relatively higher densities of pelagic (algal) resources and primary consumers (zooplankton) in early winter, allowing certain zooplankton taxa to accumulate high-quality, algal-derived fatty acids, such as DHA, during a critical seasonal transition. Algal-derived fat storage may in turn sustain such zooplankton taxa as they (fully or partly) fast in the winter months. Thus, longer-term winter survival in consumers appears to be constrained by their physiological capacities and life-history traits, including building high-quality lipid stores while exhibiting a heightened tolerance to harsh winter environmental conditions, here observed in cyclopoid copepods (*Cyclops*) but not in the cladoceran *Bosmina*. Cross-seasonal effects of consumer overwintering include altered trophic structure after ice breakup. As shown in this study, higher densities of overwintering cyclopoid copepods in spring can exert stronger, earlier top-down control (ctrl) on the spring algal bloom. Reduced food availability for other (nonoverwintering or benthic) primary consumers may have implications for energy transfer to upper trophic levels and food web dynamics over the subsequent open-water season.

ECOLOGY

underlying mechanisms are summarized in Fig. 5. In line with recent reports, our results support that changes in light availability can have strong, rapid effects on photosynthesis in early winter (17, 40, 41), and that nanophytoflagellates such as cryptophytes can remain at high densities under ice (18, 19, 42). Although crustacean zooplankton generally maintained greater early-winter densities where ice-on was delayed, an extended access to algal resources may only promote overwintering in taxa exhibiting particular physiological capacities and life-history traits already selected for in winter (Fig. 5). In our study, both the copepod *Cyclops* and the cladoceran *Bosmina* had high biomass levels in early winter, but only the former succeeded in remaining active through winter (*SI Appendix*, Fig. S4*A* vs. S4*C*). *Cyclops* and other freshwater copepods appear to overwinter more frequently than cladocerans (12, 20, 23), likely because they express trait combinations facilitating under-ice survival [e.g., tolerance to cold and starvation stress, maintenance of low metabolism, longevity (43)]; our data suggest that building high-quality lipid stores may also be an important complementary strategy to overwinter (Fig. 5), as indicated in previous studies (20, 21, 23, 24). Importantly, our 6-mo in-field experiment uncovers a cross-seasonal cascade of increased winter survival on the structure of springtime planktonic food webs, with greater densities of overwintering zooplankton effectively exploiting the spring algal bloom after ice breakup, driving stronger, earlier top-down regulation. Overwintering may thus confer a competitive advantage to winter-active taxa (such as cyclopoid copepods) over other primary consumers, possibly disrupting spring trophic linkages. Indeed, greater initial springtime densities of actively grazing cyclopoid copepods could decouple consumer–resource interactions between pelagic algae and the nonoverwintering or benthic primary consumers that can no longer benefit from the spring algal bloom (44, 45). Therefore, increasingly later ice-on dates may have far-reaching community- and ecosystem-level consequences, notably for spring successional patterns, the timing of the clearwater phase, and energy/carbon flow across trophic levels, with potentially long-lasting effects on lake food web dynamics over the open-water season (26, 30, 46).

Our comparative analysis of FA signatures contributes to a more mechanistic understanding of the physiological strategies developed by overwintering primary consumers in early winter, highlighting the potential role of ice-onset timing and resource availability in driving fat accumulation. Our experiment demonstrates that delaying ice-on dates by only a few weeks can be sufficient to stimulate greater selective retention of algal-derived FAs, especially DHA, in zooplankton. Winter-active zooplankton possibly rely on such high-quality fat storage when algal prey become scarce later in winter (20, 23, 24). Coupling microscopy and FA profiles, our data suggest that this strategy was likely employed by the overwintering cyclopoid copepod *Cyclops*. Indeed, while *Cyclops* is known to express traits that can facilitate its survival through the ice-covered season, its comparatively low densities in controls indicate that algal availability and selective fat accumulation were also key drivers, echoing previous work on the importance of algal-derived FAs for winter-active cyclopoids and copepod DHA regulation in response to cold stress (20, 23, 36, 38, 47). Given that we could observe rapid FA trophic transfer between algae and zooplankton in early winter, later ice-cover onset could further promote overwintering in certain taxa by expanding the critical time period during which consumers can accumulate algal-derived FAs.

Although ice-covered seasons shorten over time, the timing of lake ice onset can vary from year to year (5, 7). As such, our field-based experiment was influenced by the specific winter conditions during which it occurred. First, the relatively short ice-covered season (<5 mo) has likely facilitated zooplankton overwintering. Second, the early-winter weather conditions (contributing to maintaining light availability in our enclosures) and the timing of lake ice onset were also advantageous, as a winter with substantially earlier or later ice-on could have respectively resulted in less to no overwintering or, conversely, in a widespread occurrence of overwintering zooplankton, both of which limiting our ability to detect differential responses and identify causal mechanisms. Given the interannual fluctuations in freshwater ice phenology, we suggest that the prevalence of consumer overwintering may also vary among years (i.e., enhanced when ice-covered seasons begin tardily and remain short), with changes on the order of a few weeks in the timing and duration of ice cover likely to influence biophysical processes in seasonally ice-covered environments (e.g., ref. 48).

Over half of the world's lakes freeze periodically (49), with many ecosystems at risk for substantially shorter and ice-free winters over the next decades (4, 8); yet the ice-covered season remains poorly understood in freshwater science. Our field-based experiment represents a step toward emulating warming effects on ice cover to address the consequences for lake food web winter and spring phenologies. Serving as a useful tool in global change research (50), the integration of experimental approaches into winter limnology could aid in revealing the mechanisms by which biota may cope with freshwater ice loss. Echoing recent calls (12, 13), our study further stresses the need to understand under-ice processes and organismal climate sensitivities to anticipate biotic responses to rapidly changing winters.

Materials and Methods

In-Lake Experiment. We conducted a field-based experiment using a floating platform deployed on Lac Hertel, a pristine temperate lake located at McGill University's Gault Nature Reserve (Mont St-Hilaire, QC, Canada). Lac Hertel is naturally mesotrophic, with annual total phosphorus (P) and total nitrogen (N) concentrations of ~18 μg $P{\cdot}L^{-1}$ and ~300 μg $N{\cdot}L^{-1}$, and a mean summer dissolved organic carbon (C) concentration of ~3 mg $C{\cdot}L^{-1}$. Between 19 and 24 November 2018, as Lac Hertel was progressively freezing up, we secured and filled 16 enclosures with unfiltered lake water (volume ca. 3,400 L, depth ca. 4.2 m). In the middle of each enclosure, we fixed a Hobo pendant data logger at a 1-m depth to record high-resolution light-incidence and temperature data; we secured all loggers with a PVC-based structure to maintain sensor orientation (toward the surface) throughout the experiment. As Lac Hertel completed its ice-cover formation and ice was starting to form in enclosures, we initiated our ice-cover manipulations and started sampling (i.e., day 1 of experiment); a photograph of our experimental system is shown in Fig. 1*A*. Our experiment ran for a total of 183 d, from early winter (27 November 2018; day 1) through spring (28 May 2019; day 183).

To manipulate the timing of ice-on under realistic conditions, our treatment consisted of postponing the onset of ice-cover formation within enclosures by 0 (controls), 7, 14, and 21 d, namely a regression-style design with four treatment levels and four replicates per level. A schematic representation of the experimental design is illustrated in Fig. 1 *D* and *E*. To manipulate the timing of ice-cover onset, we manually removed every freshly formed piece of ice (and snow, if any) within treated enclosures twice per day, at dawn and dusk, and stored ice pieces from each enclosure in separately assigned containers. When necessary, we used a shovel to break thin layers of ice while limiting movements as much as possible to minimize mixing within the upper water layer of enclosures. We transported ice pieces to an on-site laboratory and placed individual ice containers within a large tank partially filled with tap water at the ambient laboratory temperature (10 to 12 °C); we covered individual containers with nonhermetical lids to prevent atmospheric deposition of debris and maintain dark conditions. After a melting period of 8 to 14 h, we gently poured the ice meltwater from each container back into each corresponding enclosure. This procedure enabled maintenance of similar water volumes and chemistry across enclosures despite treatment type. Upon completion of each treatment planned-delay period, ice cover was fully and naturally formed within 24 to 36 h. However, rates of change in under-ice light attenuation varied with natural meteorological fluctuations, especially air temperature, sunlight, and, most importantly, snowfall and snow accumulation. Thus, while the timing of ice-cover onset spanned four evenly spaced dates (days 1, 8, 15, and 22), rates of under-ice light attenuation varied among enclosures with different specific ice-on dates, being typically reached fully after snowfall events and, thus, at irregular increments among treatments. Baseline observations and additional explanations regarding the efficiency of our manipulations of ice-cover formation and light availability are provided in

SI Appendix, Figs. S1 and S2 and Tables S1 and S2. In sum, light attenuation occurred relatively rapidly in enclosures where ice cover formed on days 1 and 8 (blue and yellow lines in *SI Appendix*, Fig. S1), while milder conditions between days ca. 11 and 21 delayed light attenuation in enclosures with ice-on days on day 15 (orange lines in *SI Appendix*, Fig. S1 *B* and *D*). Full light attenuation took up to ca. 40 d in enclosures where ice formed on days 15 and 22 (orange and red lines), although light availability after day 22 was higher in the latter. Consequently, greater light availability occurred over a longer period in enclosures where ice formed on day 15 (orange lines), rendering light regimes similar to enclosures where ice formed on day 22 (red lines). We further explain similarities and differences in (maximum and mean) light-incidence trends during (days 1 to 22) and after (day >22) the treatment period in a summary below *SI Appendix*, Table S1. Note that ice-cover manipulation had no effect on water temperature (*SI Appendix*, Fig. S1 *E* and *F* and Table S2), indicating that treatment effects primarily operated through variation in light availability.

Sampling and On-Site Processing. We sampled all lake enclosures and the source lake ($n = 17$ sites) on 10 occasions: days 1, 8, 15, 22, 31, 45, 81, 150, 166, and 183. This schedule included weekly samplings during the treatment period (days 1, 8, 15, 22), three punctual sampling occasions over the remainder of the ice-covered period (days 31, 45, 81), and three sampling occasions in the spring following ice breakup (days 150, 166, 183). (Note that a comparative overview of lake versus control data for main response variables is presented in *SI Appendix*, Table S6, demonstrating the ecological relevance of the temporal dynamics recorded in our enclosures.) To sample ice-covered enclosures, we made a small hole (diameter ca. 15 cm) with an ice auger, after which we immediately measured ice thickness. On each sampling day, we measured a standard suite of physicochemical parameters (conductivity, pH, temperature, and dissolved oxygen) in all 17 sites, using a YSI multiparameter sonde. We also acquired high-resolution light incidence and temperature at a depth of 1 m for 140 d (i.e., a few days prior to full ice-off) with individual loggers; loggers were deployed at the beginning of the experiment, as described previously. To corroborate the efficacy of our ice manipulations on light-incidence patterns, we also recorded light penetration along a vertical profile from subice cover to a depth of 3 m using a photometer (LI-192; LI-COR) over the first weeks of our experiment.

To assess the pelagic planktonic food web response to delayed lake ice formation, we targeted a diverse set of response biotic variables across trophic levels: 1) total chl-*a* concentrations and that of four major algal groups (see below), 2) photosynthetic and heterotrophic nanoflagellate densities (PNF and HNF, respectively), 3) crustacean and rotifer zooplankton densities, as well as 4) FA contents across zooplankton, seston (organisms and materials comprised within the 0.7- to 53-μm range), and dissolved organic matter (the latter being excluded from the present study). The three first response variables were used to reconstruct food web dynamics and trophic structure from early winter to spring, including metabolic shifts from autotrophy to heterotrophy at the base of the food chain (NFs), while the use of FAs enabled the assessment of winter strategies in early winter through the comparison of fat-storage composition and energy/dietary sources sustaining primary consumers. For biotic measurements, we collected water samples using a 2-L vertical water sampler (Kemmerer; Cole Parmer). We sampled equal volumes of water at standardized depths; we avoided sampling the last meter of our enclosures owing to potential accumulations of sedimented biological materials or suspended debris. The total volume of collected water per enclosure varied with the number of variables sampled, from 2 to 14 L; a graphical representation of measurement frequencies for each biological response variable is shown in Fig. 1*E*. We stored water samples in assigned lightproof 20-L carboys (wrapped with dark, opaque plastic) and performed all subsampling steps in the on-site laboratory, as it was impossible to manipulate water samples without freezing in the field under subzero winter conditions. Subsampling and on-site processing steps were as follows:

1) Total and group-specific chl-*a*. On all 10 sampling occasions, we quantified chl-*a* concentration as a proxy for phytoplankton biomass. From the bulk water samples, we poured 50 mL into lightproof microcentrifuge tubes and measured chl-*a* fluorometrically using a benchtop FluoroProbe (BBE Moldaenke). Through the excitation of chl-*a* and accessory pigments, the FluoroProbe determined total chl-*a* concentration and that of four major spectral groups of algae known to differ in their pigment coloration and fluorescence, namely cryptophytes, golden/brown algae (including diatoms, dinoflagellates, chrysophytes), green algae (including chlorophytes, euglenophytes), and blue-green algae (cyanobacteria).
2) Nanoflagellates. We collected PNF and HNF samples on all but two occasions (two final time points), as changes in PNF and HNF densities following ice breakup were not the focus. From bulk water samples, we prefiltered 25 mL through a 53-μm sieve to remove large organisms, collected filtrates (<53 μm) in 30-mL Nalgene bottles, and fixed duplicate samples with glutaraldehyde (final concentration 1%) as well as three field blanks of ultrapure water. We kept all samples in the dark at 4 °C until transfer onto microscope slides.
3) Zooplankton. We collected zooplankton samples on all but two (second and third) occasions. The rationale behind this decision was to preclude oversampling populations in early winter. We sieved 6 L from bulk water samples with a 53-μm mesh, anesthetized collected zooplankton with carbonated water, and fixed samples with ethanol (final concentration 80%).
4) FAs. To characterize FA signatures at key time points over the experiment, we collected samples on four occasions for zooplankton (days 1, 22, 45, and 150; but see analytical limitations in the next section) and on six occasions for seston (days 1, 8, 15, 22, 45, and 150). For zooplankton, we sieved 6 L of water to concentrate organisms >53 μm in sterile 50-mL microcentrifuge tubes. For seston (0.7 to 53 μm), we prefiltered 500 mL of water through a 53-μm sieve and filtered filtrates (<53 μm) onto precombusted, preweighted (at 550 °C) 0.7-μm glass microfiber filters (GF/F; Whatman). We stored seston filters individually in aluminum foil. We stored all samples for the extraction of FAs at −80 °C until analysis.

Laboratory Analyses. To estimate NF densities, we first transferred organisms onto microscope slides. We filtered samples onto 25-mm, 0.6-μm polycarbonate black filters (AMD Manufacturing) in semidark conditions to minimize photodegradation. Halfway through each filtration, we added 100 μL DAPI (final concentration 5 $\mu g \cdot mL^{-1}$; Thermo Fisher), waited 10 min for cell staining, and then completed the sample filtering. Then, we gently placed filters onto microscope slides, sealed filters with coverslips while ensuring that organism-containing filter sides faced cover slides, and stored samples in standard microscope slide cases at −20 °C.

We counted PNF and HNF individuals by epifluorescence microscopy using a Nikon microscope in a darkened room to minimize photodegradation. For each sample, we counted a minimum of 400 organisms between 2 and 20 μm (i.e., NF cell-size range). We divided cell enumerations into three size categories: 2 to 5, 5 to 10, and 10 to 20 μm using an ocular micrometer. To visualize DAPI-stained cells, we used an ultraviolet-DAPI filter cube (Nikon model ET-DAPI-96360). To differentiate photosynthetic (PNF) from heterotrophic (HNF) cells, we used a blue-light filter cube (Nikon model ET-GFP-96362). When needed, we also employed a green-light filter cube to improve visual contrast and better distinguish cells (Nikon model ET-DsRD-96364). Note that for day 150, we only counted NFs for a subset of the samples, as very few PNFs were encountered and effects on PNF:HNF ratios after ice breakup were not the focus of this study.

We counted every crustacean and rotifer individual in zooplankton samples for all 17 sites of the eight sampling occasions. Note that species diversity remained low throughout winter. From November through January, we observed two dominant crustaceans: *Bosmina longirostris* (shown in Fig. 1*B*) and *Cyclops scutifer*, but only the latter prevailed in February. Rotifers were slightly more diverse but were dominated by genera *Keratella* and *Trichocerca*. In addition to being representative of the zooplankton community in Lac Hertel, these species are known to do well in field enclosures (51).

FAs were extracted from freeze-dried zooplankton and seston as described in ref. 23; this protocol allows for the conversion of lipid extracts to FA methyl esters. FA methyl esters were isolated with $KHCO_3$ (water 2% volume/volume and hexane) and characterized by gas chromatography–mass spectrometry (GC–MS), using an Agilent 7890A gas chromatograph coupled with an Agilent 5975C mass spectrometer with a triple-axis detector and an Agilent J&W DB-23 column. A mixture of methanol/toluene and acetyl chloride (4/1/0.125) was added to the samples with an internal standard (nonadecanoic acid; C19:0; N5252, Sigma-Aldrich). After centrifugation, samples were incubated at 90 °C for 20 min. Transesterified FAs were extracted with hexane and submitted to GC–MS identification. Standards included an FA methyl ester mix (37 components, 10 mg/mL; 47885-U, Supelco), a bacterial acid methyl ester mix (47080-U, Sigma-Aldrich), methyl palmitoleate (76176, Fluka), *trans*-11-vaccenic methyl ester (46905-U, Sigma-Aldrich), methyl stearidonate (43959, Fluka), and 9(*Z*)-eicosenoic acid methyl ester (20-2001-1, Cedarlane). Seston FAs were extracted for all samples. For zooplankton, FAs could not be extracted from four samples collected on day 45, as well as all samples from day 150, owing to loss of samples; thus, no FA data could be reported for zooplankton on day 150.

Data Manipulation and Statistical Analysis.

Temporal dynamics of planktonic food webs. To enable comparisons among plankton response variables, we converted crustacean, rotifer, and NF abundances to biomass. For rotifers and crustaceans, we used taxon-specific dry mass estimates compiled in refs. 52 and 53; a list of conversion factors for

ECOLOGY

species from Lac Hertel is provided in ref. 51. We estimated NF biomass from cell counts in three cell-size classes. We first assigned an average cell diameter of 3.5, 7.5, and 15 μm for each size class (2 to 5, 5 to 10, and 10 to 20 μm, respectively) and estimated NF biovolumes assuming spherical shapes; we then converted biovolumes to C mass units (μg $C{\cdot}L^{-1}$) using a factor of 0.22 pg $C{\cdot}\mu m^{-3}$ (54). We explored trends in PNF, HNF, and PNF:HNF mass ratios, but focus on the latter in our main results.

Statistical analyses were performed in R version 4.0.0 (55). We applied a $\log_{10}(1+X)$ transformation on biotic response variables (chl-*a*, NFs, rotifers, and crustaceans) and their mass ratios in our analyses. We quantified the main and interaction effects of ice-cover manipulation (ice-on dates) and time (day of experiment) on biotic response variables. Given the time dependence of effects (both in magnitude and direction; e.g., reversed effects on chl-*a* during spring), we treated ice-on date as a continuous variable and time as a factor to fit interaction effects for each sampling day. We quantified effects as of day 22, namely upon completion of all treatments. To account for pseudoreplication (nonindependence) across temporally repeated measurements from the same enclosures, we built LMMs for each response variable, with the function *lmer* in the R package *lme4*, and set "individual enclosure" as a random effect. We scaled model coefficients (parameter estimates) to adequately compare effect sizes among types of response variables, and plotted scaled effect sizes for each sampling day using the *sjplot* and *ggplot2* packages in R. To test for cascading effects of our ice-cover manipulation on springtime planktonic food webs (i.e., on days 150, 166, and 183 of the experiment), both between and within trophic levels, we calculated consumer–resource and consumer–consumer mass ratios across taxa and used LMMs with an identical model structure as previously described.

FA signatures. To explore how FA composition varied across enclosures after delaying ice-cover onset, we built a series of ordinations using all 40 quantified FAs on days 22 and 45. We performed an NMDS with a Euclidean dissimilarity index, using the *metaMDS* function in the R package *vegan*. To accommodate differences in distributions between zooplankton and seston FA data, we analyzed data separately and applied a log-based transformation as per ref. 56 on the former and a Wisconsin transformation on the latter. We only retained NMDS ordinations with stress values inferior to 0.18. Then, we used a PERMANOVA to determine whether FA composition varied across enclosures with different ice-on dates. This analysis was implemented using the *adonis* function in the R package *vegan*, with a permutation number fixed at 999.

To investigate winter survival strategies in zooplankton, we tracked the source of energy accumulated in seston and zooplankton using FAs as biomarkers. Building on previous studies using FAs as biomarkers, we classified FAs based on whether they were derived from algal, terrestrial, or bacterial biosynthesis. Compiling data from refs. 23, 38, 57, and 58 and references therein, we identified the origin of 23 FAs out of the 40 FAs quantified. Briefly, algal biomarkers consisted of unsaturated FAs (C16:1n7, C18:2n6, C18:3n3, C18:3n6, C18:4n-3, C20:1n-9, C20:2n6, C20:3n3, C20:3n6, C20:4n-6, C20:5n-3, C22:6n-3, C24:1n-9), terrestrial biomarkers consisted of long-chained saturated FAs (C20:0, C22:0, C23:0, C24:0), while bacterial biomarkers included branched-chain saturated FAs (a-C15:0, i-C15:0, i-C16:0, i-C17:0) and other saturated FAs (C15:0, cyclic C17:0). For both zooplankton and seston, we examined variation in total amounts and proportions (% relative to total FAs) of source-specific biomarkers. We also specifically assessed the response of three essential, algal-derived FAs (59) known to be associated with seasonal physiological regulation in zooplankton (36, 38, 60): DHA, ARA, and EPA. To quantify effects (both in strength and direction) with increasing treatment intensity on days 22 and 45, we used linear regression models with ice-on dates as a continuous variable. ANOVAs with ordered factors were also explored but discarded from main analyses so as to more fully exploit the regression nature of our design and better cope with unbalanced subsets of data resulting from missing values on day 45.

Next, we explored relationships between seston and zooplankton FA components (source-specific biomarkers, DHA, EPA, and ARA) as an indication of 1) trophic transfer from seston to zooplankton (61) and 2) under-ice survival strategies in zooplankton (i.e., strategies related to particular dietary supply or the retention of specific FAs). As a complement to linear models, we also performed a principal-component analysis (PCA) to assess seston–zooplankton FA relationships from a multivariate perspective, with the function *rda* in the R package *vegan*. We built the PCA using all seston and zooplankton source-specific biomarkers, DHA, EPA, and ARA, and examined correlations between seston and zooplankton FA components (angles among vectors) with a type 2 scaling. The multivariate correlation analysis did not reveal any patterns other than what had been previously uncovered by our linear models (*SI Appendix*, Fig. S6 and Table S3) and was thus excluded from the main results.

Data Availability. The environmental (light, temperature), FA (seston, zooplankton), and biomass (phytoplankton, zooplankton) data reported in this paper have been deposited in Figshare (62): https://doi.org/10.6084/m9.figshare.16934659.v4.

ACKNOWLEDGMENTS. We thank the staff of the Gault Nature Reserve and the interns of the Nature Conservancy (James Mager, Lena Dietz Chiasson, and Michelle Parry) for their invaluable help in the field. We acknowledge the Centre de la Nature for its daily assistance with our daily ice manipulations. We express our most sincere thanks to everyone who braved the cold to set up this experiment and sample in the winter of 2018 to 2019 (Eyerusalem Goitom, Emeric Mahé, Pascale Caissy, Kaushar Kagzi, Charles Bazerghi, Egor Katkov, Cynthia Soued, Inès Levade, and Alex Arkilanian), as well as during our trials in the winter of 2016 to 2017 (Vincent Fugère, Cindy Paquette, Richard LaBrie, Alexandre L. Bourassa, Charlotte Begouen, Anna Potapova, Kristen Hogg, Lindsay Meehan, Flavia Papini, and others previously named). We are thankful to Maxime Čapkun-Huot, Capucine Lechartre, Olympe Durrenberger, Katherine Velghe, Marilyne Robidoux, Pierre Carrier-Corbeil, and Balla Sylla for their assistance with laboratory work. M.-P.H. was supported by doctoral fellowships from the Natural Sciences and Engineering Research Council (NSERC) and Fonds de Recherche du Québec Nature et Technologies, as well as a Philanthropic Educational Organization–Sisterhood scholar award for women medical and doctoral students. This work was funded through a National Geographic Grant for Early-Career Researchers (CP-094ER-17) and a Student Research Prize from the American Society of Naturalists (to M.-P.H.), as well as through individual NSERC Discovery Grants (to M.R., G.F.F., and B.E.B.). The experimental facility was funded through an NSERC Research Infrastructure Grant (to G.F.F. and B.E.B.). M.-P.H. acknowledges support from the Department of Biology at McGill University for travel expenses.

1. C. M. O'Reilly *et al.*, Rapid and highly variable warming of lake surface waters around the globe. *Geophys. Res. Lett.* **42**, 10773–10781 (2015).
2. P. Schneider, S. J. Hook, Space observations of inland water bodies show rapid surface warming since 1985. *Geophys. Res. Lett.* **37**, 22405–22409 (2010).
3. J. J. Magnuson *et al.*, Historical trends in lake and river ice cover in the Northern Hemisphere. *Science* **289**, 1743–1746 (2000).
4. S. Sharma *et al.*, Widespread loss of lake ice around the Northern Hemisphere in a warming world. *Nat. Clim. Chang.* **9**, 227–231 (2019).
5. B. J. Benson *et al.*, Extreme events, trends, and variability in Northern Hemisphere lake-ice phenology (1855–2005). *Clim. Change* **112**, 299–323 (2012).
6. M. A. Imrit, S. Sharma, Climate change is contributing to faster rates of lake ice loss in lakes around the Northern Hemisphere. *J. Geophys. Res. Biogeosci.* **126**, e2020JG006134 (2021).
7. S. Sharma *et al.*, Direct observations of ice seasonality reveal changes in climate over the past 320–570 years. *Sci. Rep.* **6**, 25061 (2016).
8. G. A. Weyhenmeyer *et al.*, Large geographical differences in the sensitivity of ice-covered lakes and rivers in the Northern Hemisphere to temperature changes. *Glob. Change Biol.* **17**, 268–275 (2011).
9. K. Salonen, M. Leppäranta, M. Viljanen, R. D. Gulati, Perspectives in winter limnology: Closing the annual cycle of freezing lakes. *Aquat. Ecol.* **43**, 609–616 (2009).
10. S. Sharma *et al.*, Integrating perspectives to understand lake ice dynamics in a changing world. *J. Geophys. Res. Biogeosci.* **125**, e2020JG005799 (2020).
11. J. L. Campbell, M. J. Mitchell, P. M. Groffman, L. M. Christenson, Winter in northeastern North America: A critical period for ecological processes. *Front. Ecol. Environ.* **3**, 314–322 (2005).
12. S. E. Hampton *et al.*, Ecology under lake ice. *Ecol. Lett.* **20**, 98–111 (2017).
13. J. Jansen *et al.*, Winter limnology: How do hydrodynamics and biogeochemistry shape ecosystems under ice? *J. Geophys. Res. Biogeosci.* **126**, e2020JG006237 (2021).
14. S. Bertilsson *et al.*, The under-ice microbiome of seasonally frozen lakes. *Limnol. Oceanogr.* **58**, 1998–2012 (2013).
15. U. Sommer *et al.*, Beyond the plankton ecology group (PEG) model: Mechanisms driving plankton succession. *Annu. Rev. Ecol. Evol. Syst.* **43**, 429–448 (2012).
16. A. R. Hrycik *et al.*, Earlier winter/spring runoff and snowmelt during warmer winters lead to lower summer chlorophyll-*a* in north temperate lakes. *Glob. Change Biol.* **27**, 4615–4629 (2021).
17. S. L. Katz *et al.*, The "Melosira years" of Lake Baikal: Winter environmental conditions at ice onset predict under-ice algal blooms in spring. *Limnol. Oceanogr.* **60**, 1950–1964 (2015).
18. D. Özkundakci, A. S. Gsell, T. Hintze, H. Täuscher, R. Adrian, Winter severity determines functional trait composition of phytoplankton in seasonally ice-covered lakes. *Glob. Change Biol.* **22**, 284–298 (2016).
19. M. Rautio, H. Mariash, L. Forsström, Seasonal shifts between autochthonous and allochthonous carbon contributions to zooplankton diets in a subarctic lake. *Limnol. Oceanogr.* **56**, 1513–1524 (2011).
20. M.-E. Perga *et al.*, Fasting or feeding: A planktonic food web under lake ice. *Freshw. Biol.* **3**, 570–581 (2020).
21. T. Schneider, G. Grosbois, W. F. Vincent, M. Rautio, Saving for the future: Pre-winter uptake of algal lipids supports copepod egg production in spring. *Freshw. Biol.* **62**, 1063–1072 (2017).

22. H. A. Vanderploeg *et al.*, Plankton ecology in an ice-covered bay of Lake Michigan: Utilization of a winter phytoplankton bloom by reproducing copepods. *Hydrobiologia* **243/244**, 175–183 (1992).
23. G. Grosbois, H. Mariash, T. Schneider, M. Rautio, Under-ice availability of phytoplankton lipids is key to freshwater zooplankton winter survival. *Sci. Rep.* **7**, 11543 (2017).
24. H. L. Mariash, M. Cusson, M. Rautio, Fall composition of storage lipids is associated with the overwintering strategy of *Daphnia*. *Lipids* **52**, 83–91 (2017).
25. C. Säwström, J. Karlsson, J. Laybourn-Parry, W. Granéli, Zooplankton feeding on algae and bacteria under ice in Lake Druzhby, East Antarctica. *Polar Biol.* **32**, 1195–1202 (2009).
26. R. Adrian, S. Wilhelm, D. Gerten, Life-history traits of lake plankton species may govern their phenological response to climate warming. *Glob. Change Biol.* **12**, 652–661 (2006).
27. L. N. de Senerpont Domis, W. M. Mooij, S. Hülsmann, E. H. van Nes, M. Scheffer, Can overwintering versus diapausing strategy in *Daphnia* determine match-mismatch events in zooplankton-algae interactions? *Oecologia* **150**, 682–698 (2007).
28. A. Donnelly, A. Caffarra, B. F. O'Neill, A review of climate-driven mismatches between interdependent phenophases in terrestrial and aquatic ecosystems. *Int. J. Biometeorol.* **55**, 805–817 (2011).
29. J. T. Kerby, C. C. Wilmer, E. Post, "Climate change, phenology and the nature of consumer–resource interactions: Advancing the match/mismatch hypothesis" in *Trait-Mediated Indirect Interactions: Ecological and Evolutionary Perspectives*, T. Ohgushi, O. J. Schmitz, R. D. Holt, Eds. (Cambridge University Press, 2012).
30. U. Sommer, A. Lewandowska, Climate change and the phytoplankton spring bloom: Warming and overwintering zooplankton have similar effects on phytoplankton. *Glob. Change Biol.* **17**, 154–162 (2011).
31. T. Woods, A. Kaz, X. Giam, Phenology in freshwaters: A review and recommendations for future research. *Ecography* **44**, 1–14 (2021).
32. K. J. Flynn *et al.*, Misuse of the phytoplankton-zooplankton dichotomy: The need to assign organisms as mixotrophs within plankton functional types. *J. Plankton Res.* **35**, 3–11 (2013).
33. M. T. Dokulil, A. Herzig, An analysis of long-term winter data on phytoplankton and zooplankton in Neusiedler See, a shallow temperate lake, Austria. *Aquat. Ecol.* **43**, 715–725 (2009).
34. J. Haberman, Comparative analysis of plankton rotifer biomass in large Estonian lakes. *Hydrobiologia* **104**, 293–296 (1983).
35. T. Virro, J. Haberman, M. Haldna, K. Blank, Diversity and structure of the winter rotifer assemblage in a shallow eutrophic northern temperate Lake Vortsjärv. *Aquat. Ecol.* **43**, 755–764 (2009).
36. M. T. Brett, D. C. Müller-Navarra, J. Persson, "Crustacean zooplankton fatty acid composition" in *Lipids in Aquatic Ecosystems*, M. T. Arts, M. T. Brett, M. Kainz, Eds. (Springer, 2009).
37. C. Twining *et al.*, The evolutionary ecology of fatty-acid variation: Implications for consumer adaptation and diversification. *Ecol. Lett.* **24**, 1709–1731 (2021).
38. B. C. McMeans, A. M. Koussoroplis, M. J. Kainz, Effects of seasonal seston and temperature changes on lake zooplankton fatty acids. *Limnol. Oceanogr.* **60**, 573–583 (2015).
39. E. Jeppesen, J. P. Jensen, M. Søndergaard, T. Lauridsen, F. Landkildehus, Trophic structure, species richness and biodiversity in Danish lakes: Changes along a phosphorus gradient. *Freshw. Biol.* **45**, 201–218 (2000).
40. A. R. Hrycik, J. D. Stockwell, Under-ice mesocosms reveal the primacy of light but the importance of zooplankton in winter phytoplankton dynamics. *Limnol. Oceanogr.* **66**, 481–495 (2021).
41. S. Song *et al.*, Under-ice metabolism in a shallow lake in a cold and arid climate. *Freshw. Biol.* **64**, 1710–1720 (2019).
42. S. D. V. Princiotta, R. W. Sanders, Heterotrophic and mixotrophic nanoflagellates in a mesotrophic lake: Abundance and grazing impacts across season and depth. *Limnol. Oceanogr.* **62**, 632–644 (2017).
43. E. Litchman, M. D. Ohman, T. Kiørboe, Trait-based approaches to zooplankton communities. *J. Plankton Res.* **35**, 473–484 (2013).
44. J. R. Griffiths *et al.*, The importance of benthic-pelagic coupling for marine ecosystem functioning in a changing world. *Glob. Change Biol.* **23**, 2179–2196 (2017).
45. M. Winder, D. E. Schindler, Climate change uncouples trophic interactions in an aquatic system. *Ecology* **85**, 2100–2106 (2004).
46. D. Gerten, R. Adrian, Climate-driven changes in spring plankton dynamics and the sensitivity of shallow polymictic lakes to the North Atlantic Oscillation. *Limnol. Oceanogr.* **45**, 1058–1066 (2000).
47. T. Farkas, G. Nemecz, I. Csengeri, Differential response of lipid-metabolism and membrane physical state by an actively and passively over wintering planktonic crustacean. *Lipids* **19**, 436–442 (1984).
48. K. A. Warner *et al.*, How does changing ice-out affect Arctic versus boreal lakes? A comparison using two years with ice-out that differed by more than three weeks. *Water* **10**, 78 (2018).
49. C. Verpoorter, T. Kutser, D. A. Seekell, L. J. Tranvik, A global inventory of lakes based on high-resolution satellite imagery. *Geophys. Res. Lett.* **41**, 6396–6402 (2014).
50. R. I. A. Stewart *et al.*, Mesocosm experiments as a tool for ecological climate-change research. *Adv. Ecol. Res.* **48**, 71–181 (2013).
51. M.-P. Hébert *et al.*, Widespread agrochemicals differentially affect zooplankton biomass and community structure. *Ecol. Appl.* **31**, e02423 (2021).
52. A. Gsell, D. Özkundakci, M.-P. Hébert, R. Adrian, Quantifying change in plankton network stability and topology based on empirical long-term data. *Ecol. Indic.* **65**, 76–88 (2016).
53. M.-P. Hébert, B. E. Beisner, R. Maranger, A compilation of quantitative functional traits for marine and freshwater crustacean zooplankton. *Ecology* **97**, 1081 (2016).
54. K. Y. Børsheim, G. Bratbak, Cell volume to cell carbon conversion factors for a bacterivorous *Monas* sp. enriched from seawater. *Mar. Ecol. Prog. Ser.* **36**, 171–175 (1987).
55. R Development Core Team, R: A Language and Environment for Statistical Computing (R Foundation for Statistical Computing, 2021).
56. M. J. Anderson, K. E. Ellingsen, B. H. McArdle, Multivariate dispersion as a measure of beta diversity. *Ecol. Lett.* **9**, 683–693 (2006).
57. S. Taipale *et al.*, Fatty acid composition as biomarkers of freshwater microalgae: Analysis of 37 strains of microalgae in 22 genera and in seven classes. *Aquat. Microb. Ecol.* **71**, 165–178 (2013).
58. S. J. Taipale, M. J. Kainz, M. T. Brett, A low ω-3:ω-6 ratio in *Daphnia* indicates terrestrial resource utilization and poor nutritional condition. *J. Plankton Res.* **37**, 596–610 (2015).
59. M. T. Brett, D. C. Müller-Navarra, A. P. Ballantyne, J. L. Ravet, C. R. Goldman, *Daphnia* fatty acid composition reflects that of their diet. *Limnol. Oceanogr.* **51**, 2428–2437 (2006).
60. B. C. McMeans, M. A. Arts, S. Rush, A. T. Fisk, Seasonal patterns in fatty acids of *Calanus hyperboreus* (Copepoda, Calanoida) from Cumberland Sound, Baffin Island, Nunavut. *Mar. Biol.* **159**, 1095–1105 (2012).
61. D. C. Müller-Navarra, M. T. Brett, A. M. Liston, C. R. Goldman, A highly unsaturated fatty acid predicts carbon transfer between primary producers and consumers. *Nature* **403**, 74–77 (2000).
62. M.-P. Hébert, Data for "Warming winters in lakes: Later ice onset promotes consumer overwintering and shapes springtime planktonic food webs." Figshare. https://doi.org/10.6084/m9.figshare.16934659.v1. Deposited 11 April 2021.